Hemodynamic Signals Correlate Tightly with Synchronized Gamma Oscillations

Jörn Niessing, *et al.*

Science **309**, 948 (2005);
DOI: 10.1126/science.1110948

Hemodynamic Signals Correlate Tightly with Synchronized Gamma Oscillations

Jörn Niessing,[1] Boris Ebisch,[1] Kerstin E. Schmidt,[1] Michael Niessing,[1] Wolf Singer,[1] Ralf A. W. Galuske[1,2]*

Functional imaging methods monitor neural activity by measuring hemodynamic signals. These are more closely related to local field potentials (LFPs) than to action potentials. We simultaneously recorded electrical and hemodynamic responses in the cat visual cortex. Increasing stimulus strength enhanced spiking activity, high-frequency LFP oscillations, and hemodynamic responses. With constant stimulus intensity, the hemodynamic response fluctuated; these fluctuations were only loosely related to action potential frequency but tightly correlated to the power of LFP oscillations in the gamma range. These oscillations increase with the synchrony of synaptic events, which suggests a close correlation between hemodynamic responses and neuronal synchronization.

Blood oxygenation level–dependent (BOLD) imaging methods are powerful tools to investigate brain function, and they are particularly well suited for studies on the human brain (*1*, *2*). However, there is still debate about which aspects of neuronal activity are reflected by the amplitude of hemodynamic responses. BOLD responses are positively correlated with action potentials (*3*, *4*) and the amplitude of evoked potentials (*5*–*7*). The latter depends not only on the number and discharge rates of activated neurons but also on the temporal coherence of action potentials and synaptic activity (*8*). The BOLD-response may thus not only be influenced by the amplitude but also by the temporal structure of neuronal discharges. This possibility is supported by recent studies, which have shown that LFP oscillations correlate better with BOLD signals than with discharge rates (*9*, *10*) and that synaptic activity elevates BOLD signals even in the absence of action potentials (*11*).

LFP-oscillations and, thus, the temporal coherence of synaptic activity vary substantially in amplitude and frequency as a function of stimulus configurations and central states. During sleep and relaxed wakefulness, oscillations occur at low frequencies (*12*), whereas high-frequency oscillations prevail during states of arousal and focused attention (*13*, *14*). We studied the relations between hemodynamic signals, action potentials, and LFP oscillations in different frequency bands. Anesthetized adult cats were visually stimulated with moving whole-field gratings of different orientation, and electrical and hemodynamic activity in primary visual cortex was monitored simultaneously with the use of implanted microelectrodes and optical imaging of intrinsic signals at 570 and 610 nm (*1*). Variations in the amplitude of cortical responses were induced by presenting visual stimuli at two contrast levels (27 and 97% for low contrast and high contrast, respectively). In a parallel approach, spontaneous response changes were examined while stimulus contrast was kept constant at 97% and the variability of oscillatory patterns of cortical activity was enhanced by electrical activation of the mesencephalic reticular formation (MRF). Stimulation of this structure has been shown to enhance oscillatory activity in the gamma range by means of activation of cholinergic afferents from the basal forebrain (*15*, *16*). As a measure of the magnitude of hemodynamic responses, we used the signal amplitude in differential orientation maps calculated by subtraction of orientation maps from their orthogonal counterpart. The amplitude of electrical responses was assessed from the discharge frequency of multiunit activity (MUA) and the oscillatory patterning of responses from the power spectra of LFPs that were recorded from the same electrodes as the MUA (*17*).

Differential orientation maps resulting from stimulation with high-contrast gratings at 610 nm exhibited a markedly stronger signal amplitude than those obtained at low contrast. This is indicated by the enhanced contrast in the differential maps and the steeper gradients between regions responding to different orientations leading to a sharper delineation of orientation domains at high-contrast stimulation (Fig. 1A). Even though the time course of the hemodynamic responses was similar for both contrast levels, the peak amplitudes at low-contrast stimulation were on average ~31% lower ($P < 0.005$, Mann-Whitney U test) than at high-contrast stimulation (Fig. 1B). Simultaneously recorded MUA showed the typical phasic-tonic response pattern (Fig. 1C) and firing rates (averaged over the whole stimulus duration) were 28% lower with the low-contrast than with the high-contrast gratings ($P < 0.0001$, Mann-Whitney U test). The oscillatory LFP responses to both stimulus contrasts are shown in Fig. 1D. In these plots, power spectra from blocks of eight individual trials were averaged and then sorted in an ascending order according to the strength of the corresponding hemodynamic response. At both contrast levels oscillations occurred over a broad range of frequencies. However, on average, low-contrast stimuli evoked oscillatory responses at lower frequencies than did the high-contrast stimuli, which included predominantly oscillations in the upper gamma frequency range between 50 and 90 Hz (Fig. 1D). Interestingly, this relation also holds for responses evoked by stimuli of equal contrast. Neuronal responses in trial blocks associated with strong optical signals tended to oscillate at higher frequencies (Fig. 1D). Correlation analysis between hemodynamic signals and neuronal responses calculated across all trials and both contrast levels revealed a moderate correlation with spike rate ($r = 0.53$, Fig. 1E) and a somewhat stronger relation ($r = 0.6$, Fig. 1F) with the relative power of oscillations in the upper gamma band.

We also found a marked variability of hemodynamic responses even when contrast levels were kept constant. This variability occurred in a statelike manner in which phases of strong hemodynamic responses alternated with phases of weaker hemodynamic responsiveness. Thus, we kept the stimulus contrast constant at 97% and recorded electrophysiological and optical responses at 610 nm over several hours. For quantitative analysis, blocks of averaged results from eight repetitions of the eight different stimuli (*17*), which had been used for calculation of the hemodynamic responses, were grouped in three classes according to the strength of the respective optical response, and both optical and electrophysiological response variables were averaged within these groups. The peak amplitudes of the averaged hemodynamic responses differed significantly between the three groups. There were also marked differences in response duration; the larger responses decayed more slowly and lasted longer (Fig. 2A). Interestingly, the range of variability of hemodynamic response strength was as large as the range covered by responses evoked at different stimulus intensities (compare Figs. 1D and 2C). Neuronal firing rates also varied considerably between trials and these variations were related to the fluctuations of the hemodynamic responses (Fig. 2B). However, averaged firing rates differed only between the group with strong hemodynamic responses and the groups of medium and low response strength but not

[1]Max Planck Institute for Brain Research, 60528 Frankfurt/M., Germany. [2]Department of Biology, Technical University of Darmstadt, 64283 Darmstadt, Germany.

*To whom correspondence should be addressed. E-mail: galuske@mpih-frankfurt.mpg.de

between the latter two. By contrast, a clear difference between all three groups of hemodynamic responses existed with respect to the frequency distribution of the respective oscillatory responses in the LFPs. Low-frequency oscillations in the delta-, theta- and the alpha-frequency band (Fig. 2C) were most prominent in trial fraction 1, containing the trials with the weakest optical signal. The weakest high-frequency oscillations were observed in this fraction. With increasing hemodynamic response strength (trial fraction 2) oscillation frequency shifted from the theta and alpha band to the beta and lower gamma frequency band, and the strongest hemodynamic responses (trial fraction 3) were associated with the most prominent oscillations in the lower and upper gamma frequency band.

Figure 3A summarizes the relations between the strength of hemodynamic responses at 610 nm and the oscillation power in different LFP frequency bands for the entire data set. Low frequency activity in the delta band showed a strong negative relation with hemodynamic signal strength (r_{delta} = –0.44), whereas theta, alpha, and beta activities were more or less uncorrelated with this signal (r_{theta} = –0.23, r_{alpha} = –0.03, r_{beta} = 0.18). A weak positive relation existed for activity in the lower gamma band (r_{gamma1} = 0.33), and a strong positive correlation for oscillations in the upper gamma band (r_{gamma2} = 0.64). These relations were similar for trials without (Fig. 3A, black dots) and with MRF activation (Fig. 3A, gray dots). Optical signals measured at 570 nm exhibited a significant positive relationship exclusively with oscillations in the upper gamma band (Fig. 3B, r_{gamma2} = 0.5). In contrast, the correlation between firing rates and the optical signal at 610 nm was very low (r = 0.19) (Fig. 3C and fig. S2). At individual recording sites, firing rates usually varied with variations of the corresponding hemodynamic responses, but these correlations could be both positive and negative (r values ranging from –0.49 to 0.74). A consistent positive correlation was found for only 25% of the recording sites (r > 0.35). We also correlated firing rates with the power of gamma oscillations on a trial-by-trial basis and did not find a consistent relation (fig. S3).

The experiments with gratings of different contrast confirm the previous view that hemodynamic responses are positively correlated with stimulus intensity (*18*) and neuronal discharge rate (*4*, *9*). Moreover, the analysis of LFP oscillations revealed that stronger stimuli shifted the frequency of LFP oscillations to higher values and that there is a particularly tight correlation between hemodynamic responses and LFP oscillations in the high gamma frequency range. The present findings closely link hemodynamic responses to the processes leading to LFP oscillations in the gamma frequency range. Both aspects that contribute to the BOLD signal, blood volume changes (*19*) and changes in the deoxygenation status of hemoglobin (*20*), are positively correlated to the occurrence of gamma oscillations. Thus, our results are compatible with the finding that BOLD responses correlate better with the amplitude of LFP oscillations than with the discharge rate of cortical neurons (*9*, *10*). Because LFPs predominantly reflect transmembrane currents associated with synaptic activity (*8*), it had been proposed that BOLD responses reflected input rather than output activity (*9*, *11*), a conclusion which has also been reached on the basis of theoretical assumptions on the neuronal energy budget (*21*). Our data go beyond this interpretation and suggest that the precision of synchronous firing of neurons within a cortical volume critically contributes to the magnitude of the hemodynamic response. The amplitude of

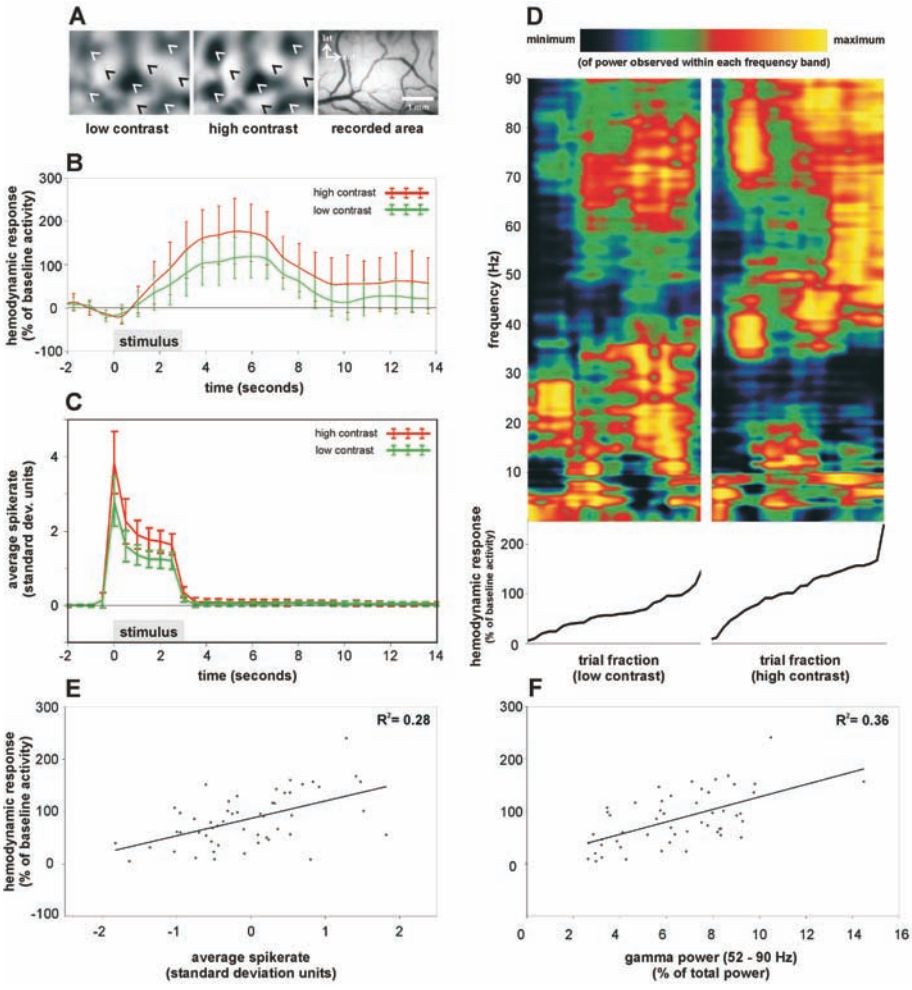

Fig. 1. Hemodynamic and electrophysiological responses to different stimulus contrasts. (**A**) Differential orientation maps representing responses to vertical (dark regions) and horizontal gratings (bright regions) at low-contrast (left) and high-contrast (right) stimulation recorded at 610 nm. For these maps, data were averaged over five recording blocks. In both maps, gray levels correspond to the same activity levels. The rightmost image depicts the recorded area. Black and white arrowheads in the activity maps indicate corresponding regions. In the recorded area, lateral (lat) is toward the top and anterior (ant) is toward the right. Scale bar, 1 mm. (**B**) Time course of the hemodynamic responses at 610 nm averaged over 26 recording blocks for each contrast level. (**C**) Peristimulus time histograms calculated from the normalized spike rate averaged over all recording blocks and sites (26 blocks, four recording sites). Error bars in (B) and (C) show means ± SD. (**D**) Power spectra of all trials (n = 26 recording blocks) sorted in an ascending order according to the hemodynamic response strength at 610 nm for each contrast level. The power of each frequency bin was renormalized to the range between the maximum and minimum power observed throughout all trials and over both contrast levels in the respective frequency bin. A low-pass filter was applied on every single frequency bin of the resulting plot (kernel size includes 10 trials). (**E** and **F**) Correlation analysis between hemodynamic responses and spike rates (E) and hemodynamic responses and gamma power in the upper frequency range (F), calculated on the basis of individual data blocks of eight stimulus presentations summarizing data from both contrast levels. Each point reflects the averaged response over eight repetitions of the presentation of the eight different stimuli. Therefore, each point reflects the average of 64 responses measured over a period of about 19 min.

LFPs depends not only on the number of active synapses within a cortical volume but to a crucial extent on the synchronicity of the synaptic events (*8*). Because of the short duration of synaptic currents, they summate most effectively if synchronized with a precision in the millisecond range. The precision of synchronous firing is in turn positively correlated with the frequency at which synchro-

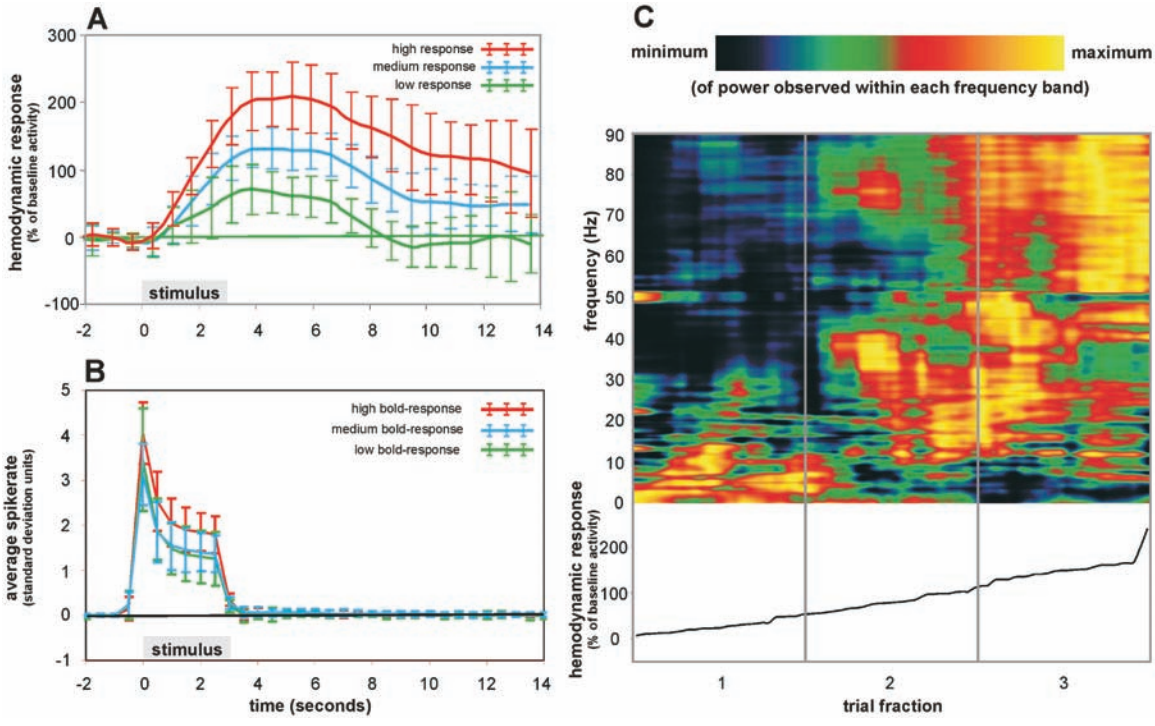

Fig. 2. Spontaneous variations of hemodynamic and electrophysiological response under conditions of constant stimulus intensity. (**A**) Time course of hemodynamic signals at 610 nm averaged over the respective 33.3% of trials with strong (red line), medium (blue line), and weak (green line) hemodynamic responses (n = 26 recording blocks for each curve). (**B**) PSTHs of the spike rates for the same trials as depicted by (A). Error bars in (A) and (B) show means ± SD. (**C**) Power spectra of all trials (n = 78 recording blocks) sorted in an ascending order according to hemodynamic response strength at 610 nm. The observed minimum and maximum activity is coded by black and yellow, respectively. A low-pass filter was applied on each single frequency bin of the resulting plot (kernel size includes 10 trials).

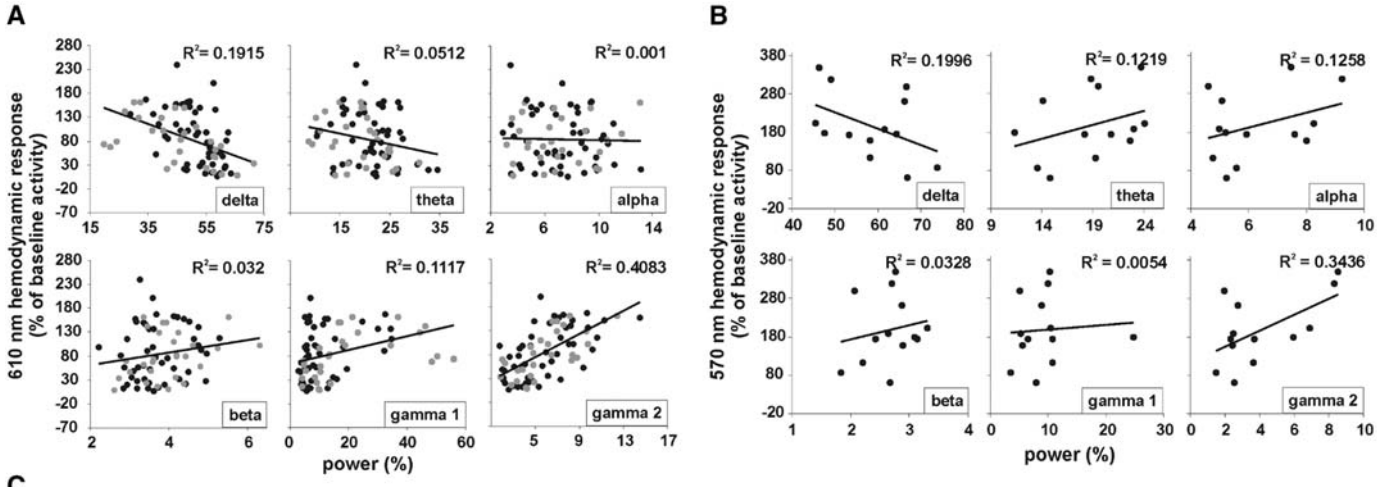

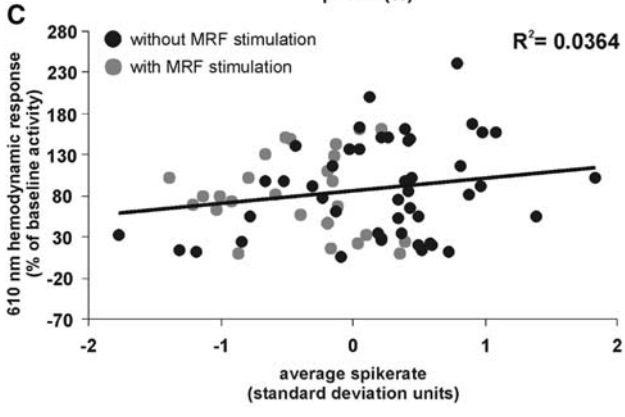

Fig. 3. Correlation analysis between hemodynamic and electrophysiological responses under constant stimulus conditions. (**A** and **B**) Scatter plots showing the relationship between hemodynamic responses obtained at 610 nm (A) and 570 nm (B) and the power in different frequency bands. (**C**) Regression plot of hemodynamic responses at 610 nm with the spike rates averaged over all normalized MUA channels.

nized groups of neurons oscillate (*15*, *22*) and reaches a maximum when cells engage in high-frequency gamma oscillations.

How do changes in the temporal patterning of responses influence hemodynamic responses? There is evidence that synchronization in the gamma frequency range is associated with oscillatory, tightly synchronized discharges of inhibitory interneurons (*23*) leading to periodic inhibition of pyramidal cells. These inhibitory postsynaptic potentials, in turn, synchronize pyramidal cells by confining their discharges to the depolarizing peaks of the membrane potential oscillations (*24*). Thus, when cortical networks engage in gamma oscillations, inhibitory interneurons are highly active, and as their discharges are phase-locked to the oscillations (*23*), their activity increases with oscillation frequency. Therefore, we propose that the hemodynamic responses associated with gamma oscillations are mainly initiated by the firing of inhibitory interneurons.

Although inhibitory interneurons constitute only about 20% of the cortical neurons, it is likely that they substantially contribute to local energy consumption. They fire at very high frequencies and distribute their numerous synapses exclusively within adjacent cortical volumes. The hypothesis that interneuron activity is a major cause of the hemodynamic response (*25*) is well compatible with the fact that interneurons contain enzymes for the synthesis of vasoactive compounds such as NO and vasoactive peptides (*26*, *27*). In this cascade, the elevated calcium concentration is suggested to play a major role (*25*).

This interpretation resolves some of the discrepancies between BOLD studies and unit recordings. Deficits in visual processing in amblyopia are well reflected by evoked potentials and hemodynamic responses, although they are undetectable in discharge rates (*7*). Attentional shifts in the absence of sensory stimulation (*28*) and mental imagery (*29*) are associated with BOLD responses, and these cognitive processes are associated with increased oscillatory activity in the gamma frequency band (*14*, *30*). Other cognitive and executive functions such as figure-ground segmentation, expectancy, sensory-motor coordination, short-term memory, and movement preparation are associated with enhanced oscillatory activity in the beta and gamma frequency range (*31*, *32*). Hemodynamic responses may thus be ideally suited to visualize neural processes associated with higher cognitive and executive functions.

References and Notes

1. R. D. Frostig, E. E. Lieke, D. Y. Ts'o, A. Grinvald, *Proc. Natl. Acad. Sci. U.S.A.* **87**, 6082 (1990).
2. S. Ogawa, T. M. Lee, A. R. Kay, D. W. Tank, *Proc. Natl. Acad. Sci. U.S.A.* **87**, 9868 (1990).
3. G. Rees, K. Friston, C. Koch, *Nat. Neurosci.* **3**, 716 (2000).
4. A. J. Smith *et al.*, *Proc. Natl. Acad. Sci. U.S.A.* **99**, 10765 (2002).
5. O. J. Arthurs, E. J. Williams, T. A. Carpenter, J. D. Pickard, S. J. Boniface, *Neuroscience* **101**, 803 (2000).
6. S. Sheth *et al.*, *Neuroimage* **19**, 884 (2003).
7. K. E. Schmidt, W. Singer, R. A. Galuske, *J. Neurophysiol.* **91**, 1661 (2004).
8. U. Mitzdorf, W. Singer, *Exp. Brain Res.* **33**, 371 (1978).
9. N. K. Logothetis, J. Pauls, M. Augath, T. Trinath, A. Oeltermann, *Nature* **412**, 150 (2001).
10. C. Kayser, M. Kim, K. Ugurbil, D. S. Kim, P. Konig, *Cereb. Cortex.* **14**, 881 (2004).
11. C. Mathiesen, K. Caesar, N. Akgoren, M. Lauritzen, *J. Physiol.* **512**, 555 (1998).
12. D. A. McCormick, T. Bal, *Annu. Rev. Neurosci.* **20**, 185 (1997).
13. M. Steriade, *Science* **272**, 225 (1996).
14. P. Fries, J. H. Reynolds, A. E. Rorie, R. Desimone, *Science* **291**, 1560 (2001).
15. S. Herculano-Houzel, M. H. Munk, S. Neuenschwander, W. Singer, *J. Neurosci.* **19**, 3992 (1999).
16. R. Rodriguez, U. Kallenbach, W. Singer, M. H. Munk, *J. Neurosci.* **24**, 10369 (2004).
17. Materials and methods are available as supporting material on *Science* Online.
18. G. M. Boynton, S. A. Engel, G. H. Glover, D. J. Heeger, *J. Neurosci.* **16**, 4207 (1996).
19. O. J. Arthurs, S. Boniface, *Trends Neurosci.* **25**, 27 (2002).
20. N. Pouratian *et al.*, *Magn. Reson. Med.* **47**, 766 (2002).
21. D. Attwell, S. B. Laughlin, *J. Cereb. Blood Flow Metab.* **21**, 1133 (2001).
22. M. Volgushev, M. Chistiakova, W. Singer, *Neuroscience* **83**, 15 (1998).
23. R. D. Traub, M. A. Whittington, I. M. Stanford, J. G. Jefferys, *Nature* **383**, 621 (1996).
24. R. Azouz, C. M. Gray, *J. Neurosci.* **19**, 2209 (1999).
25. M. Lauritzen, *Nat. Rev. Neurosci.* **6**, 77 (2005).
26. J. G. Valtschanoff *et al.*, *Neurosci. Lett.* **157**, 157 (1993).
27. B. Cauli *et al.*, *J. Neurosci.* **24**, 8940 (2004).
28. S. Kastner, M. A. Pinsk, P. De Weerd, R. Desimone, L. G. Ungerleider, *Neuron* **22**, 751 (1999).
29. S. M. Kosslyn, G. Ganis, W. L. Thompson, *Nat. Rev. Neurosci.* **2**, 635 (2001).
30. M. M. Muller, T. Gruber, A. Keil, *Int. J. Psychophysiol.* **38**, 283 (2000).
31. C. Tallon-Baudry, *J. Physiol. (Paris)* **97**, 355 (2003).
32. A. K. Engel, P. Fries, W. Singer, *Nat. Rev. Neurosci.* **2**, 704 (2001).

33. We thank H. Klon-Lipok and E. Scheibinger for technical assistance and M. Wibral, M. Lutzenburg, and G. Pipa for helpful comments and suggestions on the project.

Supporting Online Material

www.sciencemag.org/cgi/content/full/309/5736/948/DC1
Materials and Methods
Figs. S1 to S4
References

10 February 2005; accepted 10 June 2005
10.1126/science.1110948

Coupling Between Neuronal Firing, Field Potentials, and fMRI in Human Auditory Cortex

Roy Mukamel,[1] Hagar Gelbard,[1] Amos Arieli,[1] Uri Hasson,[2] Itzhak Fried,[3,4]* Rafael Malach[1]*

Functional magnetic resonance imaging (fMRI) is an important tool for investigating human brain function, but the relationship between the hemodynamically based fMRI signals in the human brain and the underlying neuronal activity is unclear. We recorded single unit activity and local field potentials in auditory cortex of two neurosurgical patients and compared them with the fMRI signals of 11 healthy subjects during presentation of an identical movie segment. The predicted fMRI signals derived from single units and the measured fMRI signals from auditory cortex showed a highly significant correlation ($r = 0.75$, $P < 10^{-47}$). Thus, fMRI signals can provide a reliable measure of the firing rate of human cortical neurons.

A major concern in the rapidly expanding field of functional magnetic resonance imaging (fMRI) has been the absence of a quantitative relationship between blood oxygenated level–dependent (BOLD) fMRI signals and neuronal activity. Several studies have attempted to characterize this relationship (*1*–*10*). In anesthetized monkeys, a higher correlation of the fMRI signal to the local field potential (LFP) was found compared with spike activity (*11*). However, the implications of these studies to the awake, conscious human brain are unclear.

Recently, we reported that movie stimuli are particularly effective in producing a widespread and robust correlation in the evoked fMRI signals across different subjects (*12*). Here, we used this phenomenon of intersubject correlation to examine the nature of the coupling between fMRI signals and neuronal activity in the sensory cortex of alert humans.

We recorded from 53 single neurons in Heschl's gyrus (auditory cortex) of two native English-speaking patients with epilepsy monitored with intracranial depth electrodes for potential surgical treatment (*13*). Recordings were done while the patients saw two repetitions of a 9-min segment from a popular

[1]Department of Neurobiology, Weizmann Institute of Science, Rehovot 76100, Israel. [2]Center for Neural Science, New York University, New York, NY 10003, USA. [3]Division of Neurosurgery, David Geffen School of Medicine, and Semel Institute for Neuroscience and Human Behavior, University of California Los Angeles (UCLA), Los Angeles, CA 90095, USA. [4]Functional Neurosurgery Unit, Tel Aviv Medical Center and Sackler School of Medicine, Tel Aviv University, Tel Aviv 69978, Israel.

*To whom correspondence should be addressed. E-mail: rafi.malach@weizmann.ac.il (R.M.); ifried@mednet.ucla.edu (I.F.)